The Sanriku-Oki low-seismicity region on the northern margin of the great 2011 Tohoku-Oki earthquake rupture

Lingling Ye,[1] Thorne Lay,[1] and Hiroo Kanamori[2]

Received 3 September 2011; revised 19 November 2011; accepted 12 December 2011; published 10 February 2012.

[1] We examine a region of the megathrust fault offshore of northeastern Honshu (38.75°–40.25°N, 141.5°–143.25°E) that we designate as the Sanriku-Oki low-seismicity region (SLSR). The SLSR, located near the northern termination of the 2011 Tohoku-Oki (M_w 9.0) rupture, lacks historical great earthquake ruptures and has relatively low levels of moderate-size ($M_j \geq 5.0$) earthquakes, with subregions having many small events (M_j 2.5–5.0) in the Japan Meteorological Agency unified catalog. The SLSR is located downdip along the megathrust from the rupture zone of the great 1896 Sanriku tsunami earthquake and the great 1933 Sanriku outer trench slope normal-faulting event; weak seismic coupling of the SLSR had been deduced based on the occurrences of those unusual events. Relatively low slip deficit on the SLSR megathrust was estimated based on GPS deformations prior to 2011 compared with adjacent areas with strong inferred locking to the south and north. The southern portion of the SLSR appears to have had, at most, modest levels (<5 m) of coseismic slip during the 2011 event. Some thrust-faulting aftershocks did occur in the SLSR, primarily at depths near 40 km where there had previously been small (M_j ~5.0) repeating earthquakes (e.g., the Kamaishi repeater). An $M_w \sim 7.4$ underthrusting aftershock occurred near the northeastern edge of the SLSR ~22.5 min after the great 2011 event. Postseismic convergence along the megathrust is peaked in the SLSR. The collective observations indicate that the SLSR is primarily undergoing quasi-static aseismic convergence, and the lack of regional strain accumulation likely delimited the northern extent of the great 2011 rupture as well as the downdip extent of the 1896 rupture. The triggering of the M_w 7.4 aftershock and heightened activity in the downdip repeater regions suggest that high postseismic strain rates drove the region to have ephemerally increased seismic failure, but it appears unlikely that a great earthquake will nucleate or rupture through this region. Similar properties may exist on the megathrust near the southern end of the 2011 rupture.

Citation: Ye, L., T. Lay, and H. Kanamori (2012), The Sanriku-Oki low-seismicity region on the northern margin of the great 2011 Tohoku-Oki earthquake rupture, *J. Geophys. Res.*, *117*, B02305, doi:10.1029/2011JB008847.

1. Introduction

[2] The subduction zone megathrust fault offshore of northeastern Honshu, Japan, accommodates ~8–10 cm/yr of plate convergence with spatially varying slip behavior, ranging from quasi-static slip to slowly rupturing tsunami earthquakes to 60+ m coseismic displacements. Anticipating the nature of slip in regions of the megathrust for which we have limited seismological history has been difficult given the regional variability, and it is important to understand the distribution and nature of the diverse fault behavior. The Sanriku-Oki region of the plate boundary fault (Figure 1) (38.75°–40.25°N, 141.5°–143.25°E) has been characterized as having low seismic coupling and very uncertain potential for hosting a large earthquake because of a lack of large historic earthquake ruptures (Figure 1b) [*Kanamori*, 1972, 1977; *Earthquake Research Committee* (*ERC*), 1998; *Yamanaka and Kikuchi*, 2004], low levels of moderate-size earthquakes (Figure 1a), and the relatively low regional slip deficit inferred from several years of GPS observations [e.g., *Mazzotti et al.*, 2000; *Nishimura et al.*, 2000; *Kawasaki et al.*, 2001; *Suwa et al.*, 2006; *Hashimoto et al.*, 2009; *Loveless and Meade*, 2010].

[3] Over the past 115 years, this region has been framed on three sides (Figure 1b) by large and great earthquake ruptures on the megathrust [*ERC*, 1998; *Yamanaka and Kikuchi*, 2004]. To the north, the 1994 Sanriku-Haruka-Oki earthquake (M_w 7.6) had almost equal amounts of coseismic and postseismic moments [*Heki et al.*, 1997; *Kawasaki et al.*, 2001]; to the east (updip), the great 1896 Sanriku tsunami earthquake (M_S 7.2, M_w 8.0–8.2, M_t 8.2–8.6) [*Kanamori*, 1972; *Aida*, 1977; *Abe*, 1979; *Tanioka and Satake*, 1996]

[1]Department of Earth and Planetary Sciences, University of California, Santa Cruz, California, USA.
[2]Seismological Laboratory, California Institute of Technology, Pasadena, California, USA.

0148-0227/12/2011JB008847

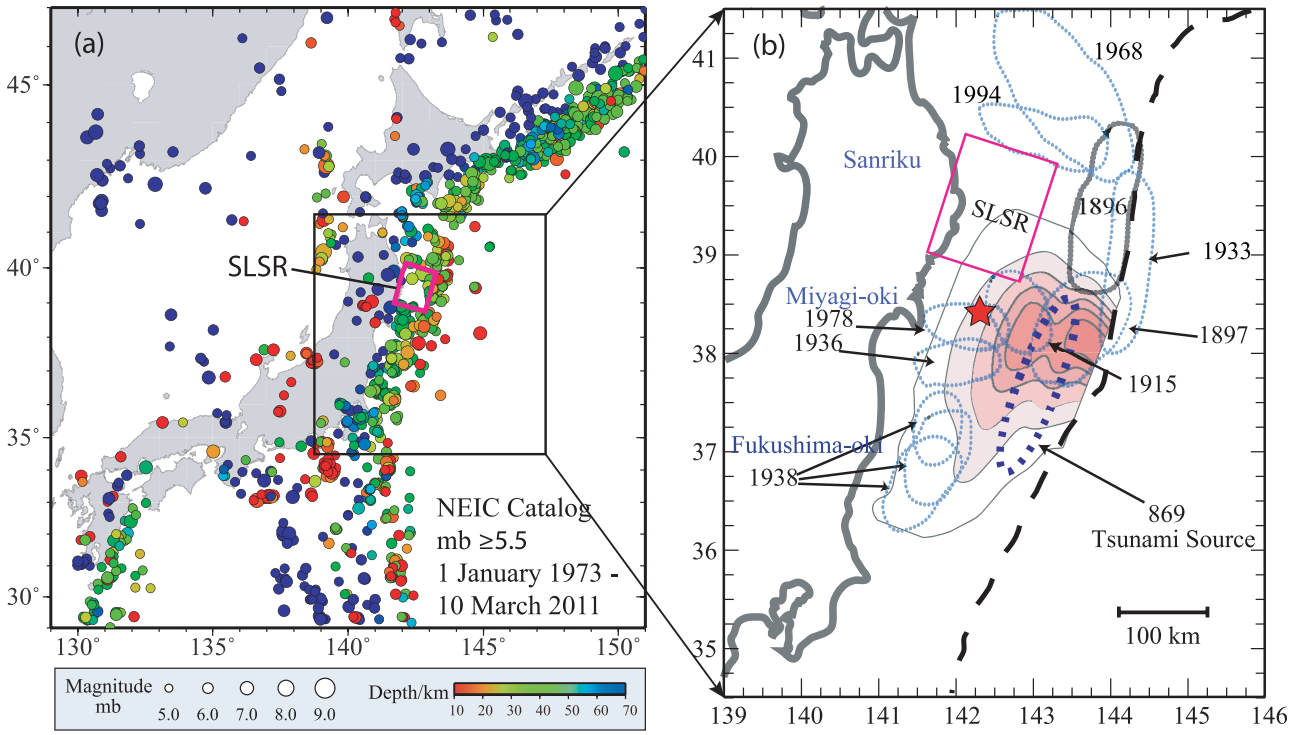

Figure 1. (a) Seismicity from the NEIC catalog around Japan from 1973 to 2011 prior to the 11 March 2011 Tohoku-Oki earthquake with $m_b \geq 5.5$. Hypocentral depths are indicated by the color scale, and symbol size increases with seismic magnitude. The magenta rectangular region indicates the SLSR. The black rectangle indicates the zoomed-in region in Figure 1b. (b) Map showing the location of the Sanriku low-seismicity region (SLSR), and schematic rupture zone of historic large earthquakes along the northeast Honshu coast [*ERC*, 1998] with blue dotted ellipsoidal shapes and a gray dotted shape for the 1896 tsunami earthquake source area [*Tanioka and Satake*, 1996] updip of the SLSR, respectively. Slip contours of 1, 10, 20, 30, 40, and 50 m for 2011 Tohoku-Oki rupture model of *Yue and Lay* [2011] are shown along with a red star for the USGS/NEIC epicentral location. The darkly dotted ellipse indicates the approximate location of the 896 Jogan tsunami source region [*Minoura et al.*, 2001]. The dashed curve indicates the position of the trench.

and the great 1933 Sanriku outer trench slope normal-faulting event (M_w ~8.6) [*Kanamori*, 1971] both generated huge tsunamis that devastated the coast of Iwate prefecture; and to the south, the sequence of large Miyagi-Ken-Oki earthquakes (M ~7.2–8.2) of 1793, 1835, 1861, 1897, 1936, 1978, and 2005 [*ERC*, 1998; *Kanamori et al.*, 2006] repeatedly ruptured the downdip portion of the megathrust. The great 2011 Tohoku-Oki earthquake (M_w 9.0) recently ruptured the entire width of the megathrust to the south with large fault displacements, particularly in the updip half of the fault zone, but limited coseismic slip appears to have occurred in the Sanriku-Oki region and many aftershocks in the area appear to be upper plate events [*Asano et al.*, 2011].

[4] While the Sanriku-Oki region has numerous small earthquakes ($M_w \leq 5.0$), as we show here, it has few moderate- to large-size events (M_w ~ 5.0–7.5) and no very large to great earthquakes ($M_w > 7.5$) in earthquake catalogs dating back to 1900 (Figure 1), so we designate it the Sanriku-Oki low-seismicity region (SLSR).

[5] The SLSR was first characterized as being nearly completely seismically decoupled in early considerations of plate coupling based on subducting plate geometry, models of subduction zone evolution, and historical earthquake behavior [e.g., *Kanamori*, 1977]. This perspective emerged from the observed along-strike variation from repeated great underthrusting earthquakes along the Kuril and Hokkaido regions to smaller, less-regular events along the Honshu coast, with the intervening 1896 tsunami earthquake, suggesting a transition in seismic coupling [*Kanamori*, 1972; *Tanioka and Satake*, 1996]. The 1896 thrust event involved large displacement of the shallow portion of the megathrust, and with no historical record of large downdip thrusting events, it is logical to infer that the deeper megathrust slips aseismically (i.e., it is seismically "decoupled"), allowing stress to build up and rupture the shallow, perhaps somewhat weakly coupled, region.

[6] This notion of decoupling of the downdip portion of the megathrust is strengthened by considering the great 1933 Sanriku normal-fault earthquake, which involved tensional fracture of the oceanic lithosphere near the trench 37 years after the 1896 tsunami earthquake [*Kanamori*, 1971]. The 1933 event is still the largest known outer trench slope normal-faulting earthquake, and it is plausible that significant loading of the plate-bending stresses by deep slab negative buoyancy was involved, again suggesting that the deep megathrust is essentially decoupled or it would have

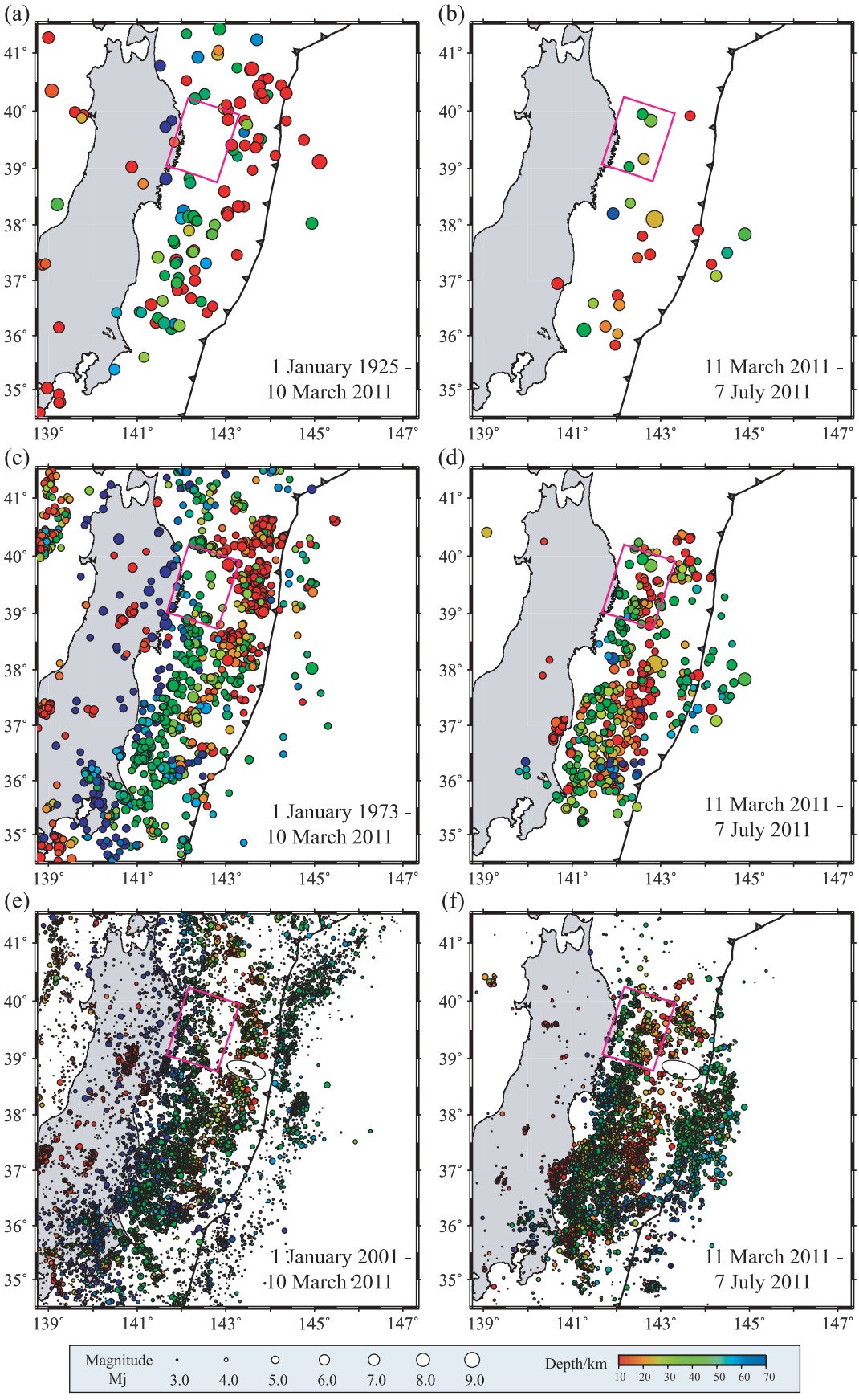
(a)
1 January 1925 -
10 March 2011
(b)
11 March 2011 -
7 July 2011
(c)
1 January 1973 -
10 March 2011
(d)
11 March 2011 -
7 July 2011
(e)
1 January 2001 -
10 March 2011
(f)
11 March 2011 -
7 July 2011
41°
40°
39°
38°
37°
36°
35°
139°
141°
143°
145°
147°
Magnitude
Mj
3.0
4.0
5.0
6.0
7.0
8.0
9.0
Depth/km
10
20
30
40
50
60
70

Figure 2

shielded the shallow plate from the deep slab pull. These ideas played a role in the widely held assessment that the Japan megathrust farther to the south was relatively unlikely to support earthquakes larger than M_w ~8.5 (estimated size of the 896 Jogan earthquake located south of the 1896 event [e.g., *Minoura et al.*, 2001]). That assessment, taken by some as an absolute upper bound on viable earthquake size, influenced earthquake hazard estimates along the Japan Trench using the characteristic earthquake model, but this perspective was evolving in the face of geodetic evidence for large megathrust slip deficits offshore of Miyagi and Fukushima prefectures [e.g., *Loveless and Meade*, 2010] and reconsiderations of the seismic history [e.g., *Minoura et al.*, 2001; *Watanabe*, 2001; *Kanamori et al.*, 2006; *Satake et al.*, 2007], and was demonstrated to be an underestimate by the great event in 2011.

[7] The rupture zones of the 1896 and 1933 earthquakes are not very well constrained, but the shallow subduction zone updip of the SLSR is seismically very active, and probable rupture regions of the earlier great events are suggested by present-day microseismicity distributions [e.g., *Gamage et al.*, 2009]. The nature of any downdip transition to aseismic displacement in the SLSR is not known in detail, but a relatively abrupt lower edge of the high-microseismicity domain is shown below.

[8] The SLSR has also been regarded as a predominantly stable sliding portion of the megathrust with small asperities that fail in small repeating earthquakes [e.g., *Igarashi et al.*, 2003; *Matsuzawa et al.*, 2002; *Matsuzawa et al.*, 2004; *Uchida et al.*, 2003]. A recurrence interval of 5.35 ± 0.53 years for $M \sim 4.7$ repeating earthquakes with very similar waveforms has been determined for the megathrust region offshore of the coastal town of Kamaishi in the downdip region of the SLSR (~39.4°N, ~142.2°E). This has been interpreted as a repeated rupture of the same asperity with a dimension of ~1 km surrounded by a creeping zone on the plate boundary [*Matsuzawa et al.*, 2002]. *Uchida and Matsuzawa* [2011] build on these observations to propose a notional hierarchical structure of asperities along the northeastern Japan coast and estimate low interplate coupling in the SLSR based on repeating earthquake analysis.

[9] During the 2011 Tohoku-Oki event, a minor slip on the order of a few meters may have occurred in the southern SLSR [*Ammon et al.*, 2011; *Lay et al.*, 2011b; *Ozawa et al.*, 2011; *Shao et al.*, 2011; *Yue and Lay*, 2011], far less than the tens of meters of slip on the megathrust to the south, but GPS data indicate that postseismic slip following the 2011 event is largest, albeit <1 m, in this region [*Ozawa et al.*, 2011]. It appears likely that the SLSR played a role in delimiting the great event's northern rupture extent. Observations of how this region, including its repeating earthquake patches, was affected by the 2011 event are relevant to seismic hazard, frictional behavior, and earthquake interactions and stress transfer on a megathrust with variable slip behavior.

[10] We use earthquake catalogs and seismic waveforms to examine the seismicity and focal mechanism of events in the SLSR in the context of it being located on the margins of the large slip zones of the 1896 and 2011 ruptures. Our attention is primarily focused on interplate thrust events, identified using as criteria event locations and regional or global centroid moment tensor (CMT) focal mechanisms.

2. Characteristics of SLSR Faulting

2.1. Seismicity and Focal Mechanisms

[11] We use the U.S. Geological Survey-National Earthquake Information Center (USGS-NEIC) preliminary determination of epicenters (PDE) catalog (1 January 1973–7 July 2011) and the Japan Meteorological Agency (JMA) unified catalog (2 January 1925–7 July 2011) to establish basic attributes of the seismicity in the SLSR. The NEIC catalog is expected to be reasonably complete for events near Japan with $m_b > 5.0$ for the 1973–2011 time interval, and some events down to $m_b \sim 2.0$ are included. The JMA unified catalog is likely to be reasonably complete back to 1925 for $M_j \geq 6.5$ and back to 1973 for $M_j \geq 5.0$. The most recent 15 years of the JMA unified catalog incorporate large numbers of observations from the high-sensitivity seismograph network (Hi-net) that was rapidly deployed after the 1995 Kobe earthquake, with the detection and completeness levels for events within the SLSR lowering with time. For the past decade, events down to $M_j \sim 2.5$ have been very well recorded in the SLSR because of its proximity to the coast. The time-varying attributes of the catalogs are complex, and we will not attempt to quantify them or differences between m_b and M_j, given that the SLSR is quite distinctive without need for any special processing. Data for two seismicity and moment tensor catalogs are presented to ensure that our interpretations do not depend on specific catalog parameters.

[12] We consider seismicity distributions prior to, and for 4 months following, the 2011 Tohoku-Oki earthquake. Before the 2011 earthquake, the framing of the SLSR by large earthquake ruptures in Figure 1b is also apparent in maps of JMA unified catalog seismicity along Honshu dating back to 1925 for large earthquakes (Figure 2a; $M_j \geq 6.5$), and back to 1973 for medium to large earthquakes (Figure 2c; $M_j \geq 5.0$). However, on the same map scale, the SLSR is not as clearly distinctive in the distribution of smaller events since 2001 ($M_j \sim 2.5$–5.0), as was noted by *Uchida et al.* [2009], although there is a somewhat sparse, patchy distribution of seismicity (Figure 2e).

[13] To date, the SLSR has hosted numerous aftershocks of the 11 March 2011 great earthquake with $M_j \geq 6.5$ and $M_j \geq 5.0$ (Figures 2b and 2d), and moderate numbers of smaller events, many in a well-defined north–south lineation in the upper plate in the southern SLSR (Figure 2f). The overwhelming task of processing the intense aftershock activity raises questions about the catalog completeness of the aftershock sequence for the lower magnitudes.

[14] The low historical seismicity for large events in the SLSR is particularly striking, given the intensity of large earthquakes at comparable downdip positions on the

Figure 2. Seismicity from the JMA unified catalog around northeast Honshu (left) prior to and (right) after the 11 March 2011 Tohoku-Oki Earthquake with (a) $M_j \geq 6.5$ from 1925 to 10 March 2011, (c) $M_j \geq 5.0$ from 1973 to 10 March 2011, (e) M_j 2.5–5.0 from 2001 to 10 March 2011. Aftershocks of the Tohoku-Oki event with (b) $M_j \geq 6.5$, (d) $M_j \geq 5.0$, and (f) M_j 2.5–5.0 up until 7 July 2011. The ellipses in the lower panels denote the "seismic gap" for small earthquakes [*Uchida et al.*, 2004]. The toothed black line indicates the Japan Trench. Other symbols are the same as those in Figure 1.

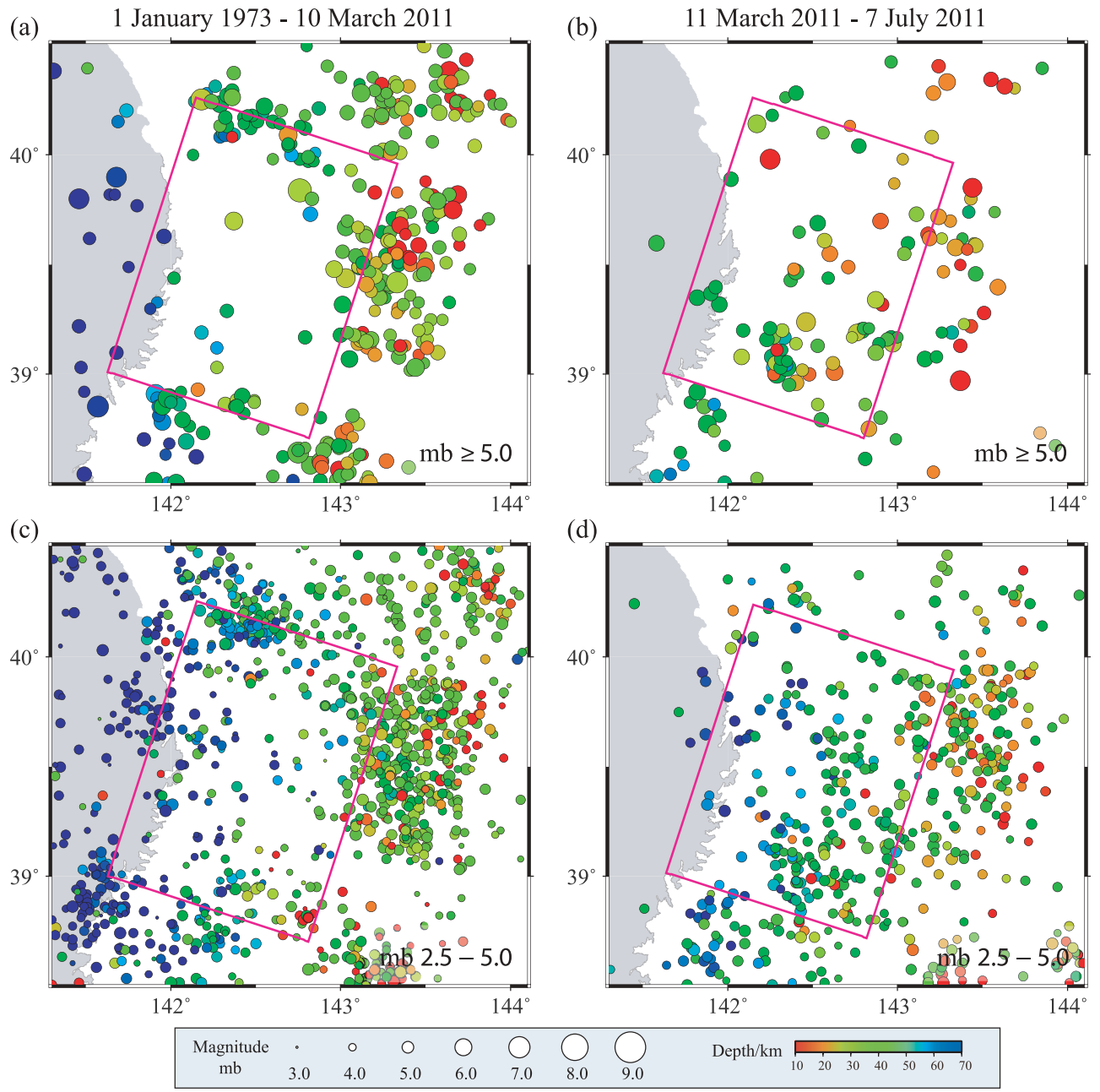

Figure 3. Seismicity from the NEIC catalog around the SLSR from 1973 to 2011 prior to the 11 March 2011 Tohoku-Oki earthquake with (a) $m_b \geq 5.0$ and (c) $m_b < 5.0$, and after the Tohoku-Oki earthquake with (b) $m_b \geq 5.0$ and (d) $m_b < 5.0$. Other symbols are the same as those in Figure 1.

megathrust to the south along the Miyagi-Ken-Oki zone. It is clear in Figures 2a and 2c that the near-trench portion of the megathrust that ruptured with large slip updip of the hypocenter in 2011 (Figure 1b) had relatively few large or small preceding events in the JMA unified catalog, and it also had few aftershocks. This is also the case in the latitude range 35°–36°N, on the southern margin of the large slip region in the 2011 event. A localized region from 38.8°–39.0°N, 143°–144°E updip from the SLSR (ellipses in Figures 2e and 2f) has very low activity at all magnitude levels, as was discussed by *Uchida et al.* [2004]. We will discuss these low-seismicity regions later, although it is clear that a relative lack of seismicity alone can be misleading with respect to seismogenic potential. Overall, the SLSR appears to have general similarities to the creeping section of the San Andreas fault, where there are many small events but no large events, and large adjacent ruptures do not seem to be able to penetrate through the region [e.g., *Wyss et al.*, 2004].

[15] We now zoom in on the SLSR and examine the regional seismicity in more detail. The updip portion of the megathrust extends to ~144°E, near the trench. The NEIC catalog (Figure 3a) and JMA unified catalog (Figure 4a) show that there has been much higher seismic activity for m_b or $M_j \geq 5.0$ since 1973 in the updip portion of the megathrust, where the 1896 earthquake rupture occurred. Both catalogs indicate a transition in seismicity levels near

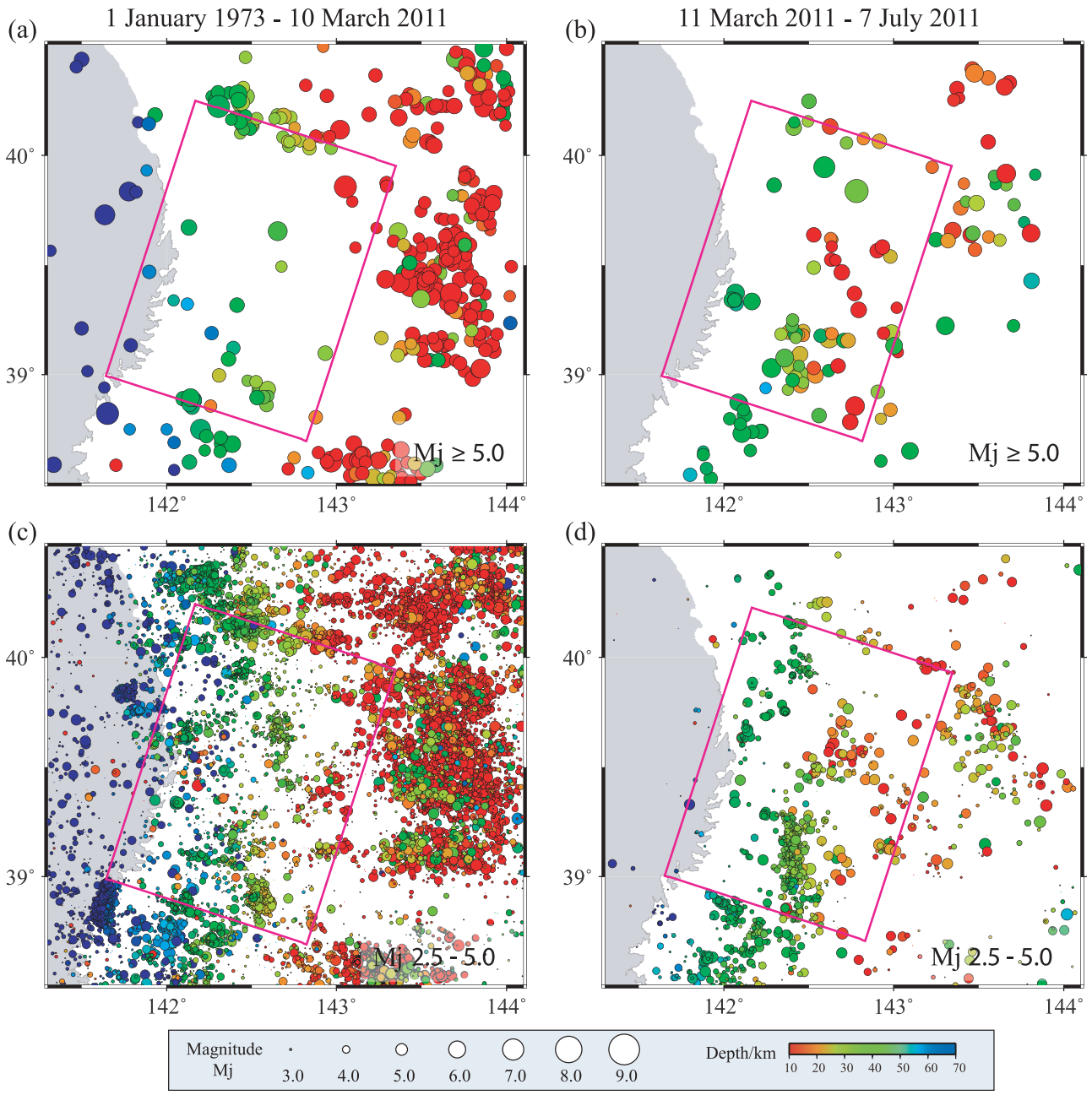

Figure 4. Seismicity from the JMA unified catalog around the SLSR from 1973 to 2011 prior to the 11 March 2011 Tohoku-Oki earthquake with (a) $M_j \geq 5.0$ and (c) $M_j < 5.0$, and after the Tohoku-Oki earthquake with (b) $M_j \geq 5.0$ and (d) $M_j < 5.0$. Other symbols are the same as those in Figure 1.

~143°E or somewhat farther to the east. Because of limited teleseismic location capabilities, the NEIC catalog has moderate numbers of small earthquakes for $m_b \sim 2.5$–5.0 (Figure 3c). Many more small events (M_j 2.5–5.0) are found in the JMA unified catalog in the SLSR region from 1973 to 2011 (Figure 4c), with most of the smaller events in the catalog being since 1995. Several distinct clusters are indicated by the smaller activity, but are not as evident for the larger events. Both catalogs define the almost completely aseismic region extending to the trench within 38.8°–39°N, 143°–144°E corresponding to the ellipses in Figures 2e and 2f. This low-seismicity region, with a particularly strikingly well-defined northern edge in Figure 4c, may demark the southern limit of the 1896 rupture zone [*Aida*, 1977], although some estimates indicate a more southerly rupture limit near 38.4°N (e.g., Figure 1b) [*Tanioka and Satake*, 1996]. The aseismic region extending to the trench lies near the northern edge of the large updip slip region for the 2011 event (Figure 1b) as well.

[16] Aftershock activity in the SLSR for the 2011 Tohoku-Oki earthquake is substantial relative to the preceding several decades, as seen for both the NEIC catalog (Figures 3b and 3d) and the JMA unified catalog (Figures 4b and 4d). The differences between catalog locations for the

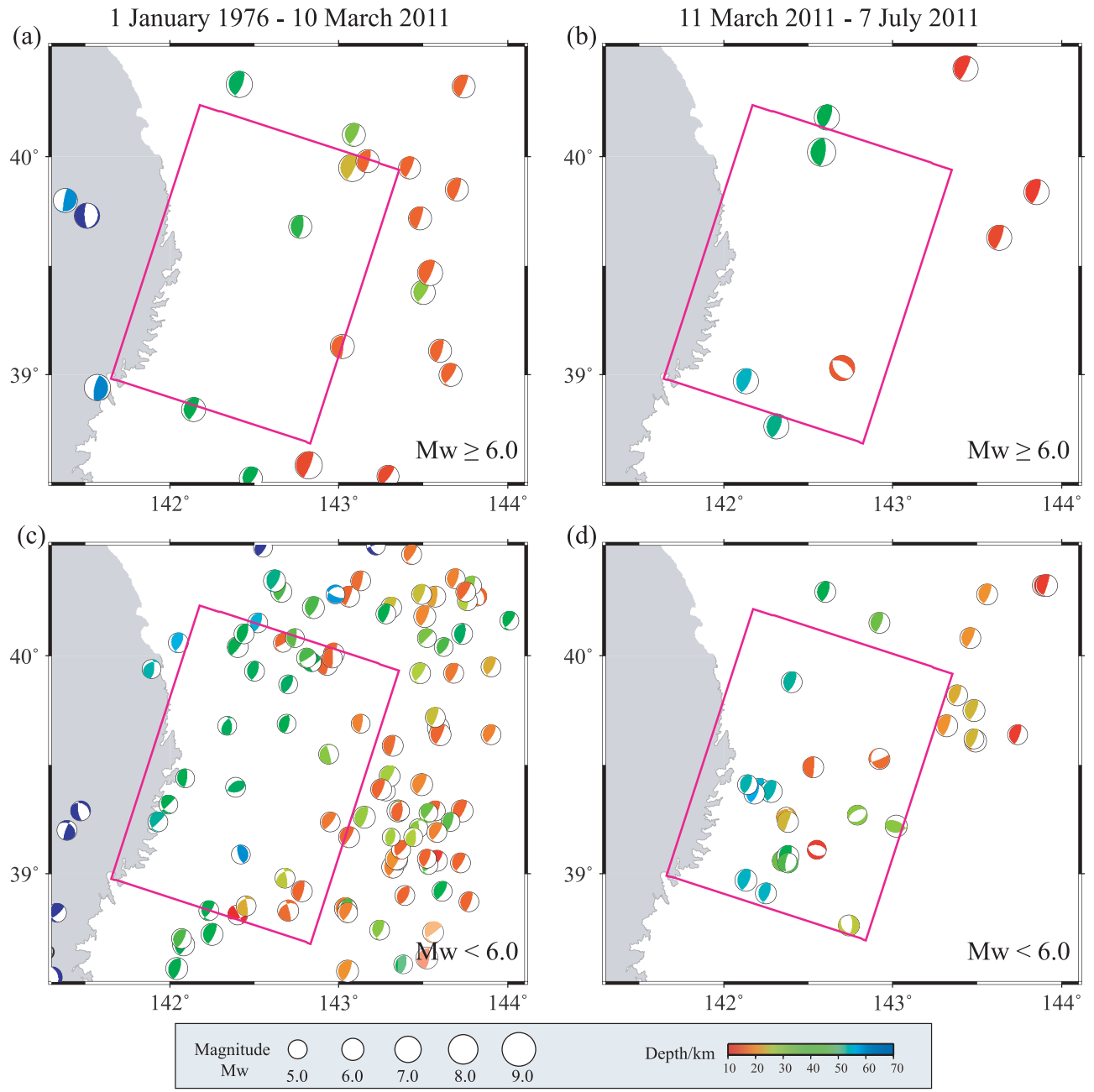

Figure 5. Focal mechanisms from the GCMT catalog around the SLSR since 1976 prior to the 11 March 2011 Tohoku-Oki earthquake with (a) $M_w \geq 6.0$ and (c) $M_w < 6.0$, and after the Tohoku-Oki earthquake with (b) $M_w \geq 6.0$ and (d) $M_w < 6.0$. Other symbols are the same as those in Figure 1.

aftershocks are clearly apparent, with larger events tending to be located farther offshore in the JMA unified catalog than in the NEIC catalog, and smaller events tending to be more clustered in the JMA unified catalog, notably for the north–south lineation apparent in Figure 4d. It is interesting that the aseismic patch near 38.9° that extends to the trench is remarkably devoid of aftershocks in the JMA unified catalog (Figures 4b and 4d), and there are regions within the SLSR that appear similarly devoid of aftershocks. As is true for the main shock rupture zone to the south, many of the aftershocks are actually shallow, upper plate events (most red symbols in the SLSR regions in Figures 3b, 3d, 4a, and 4b), and it is useful to examine aftershock focal mechanisms to help identify events on the SLSR megathrust, which is of primary interest here.

[17] We extracted all focal mechanisms in the Sanriku-Oki region from the global centroid moment tensor (GCMT) catalog back to 1976 (Figure 5) and the NIED regional CMT mechanism catalog back to 1997 (Figure 6). All available solutions are shown, separated by magnitudes less than or greater than M_w = 6.0 and by timing relative to the great 2011 Tohoku-Oki event. For the GCMT solutions, the lowest value of M_w is 4.7, and the events are plotted at the GCMT centroid locations. Most of the GCMT events around

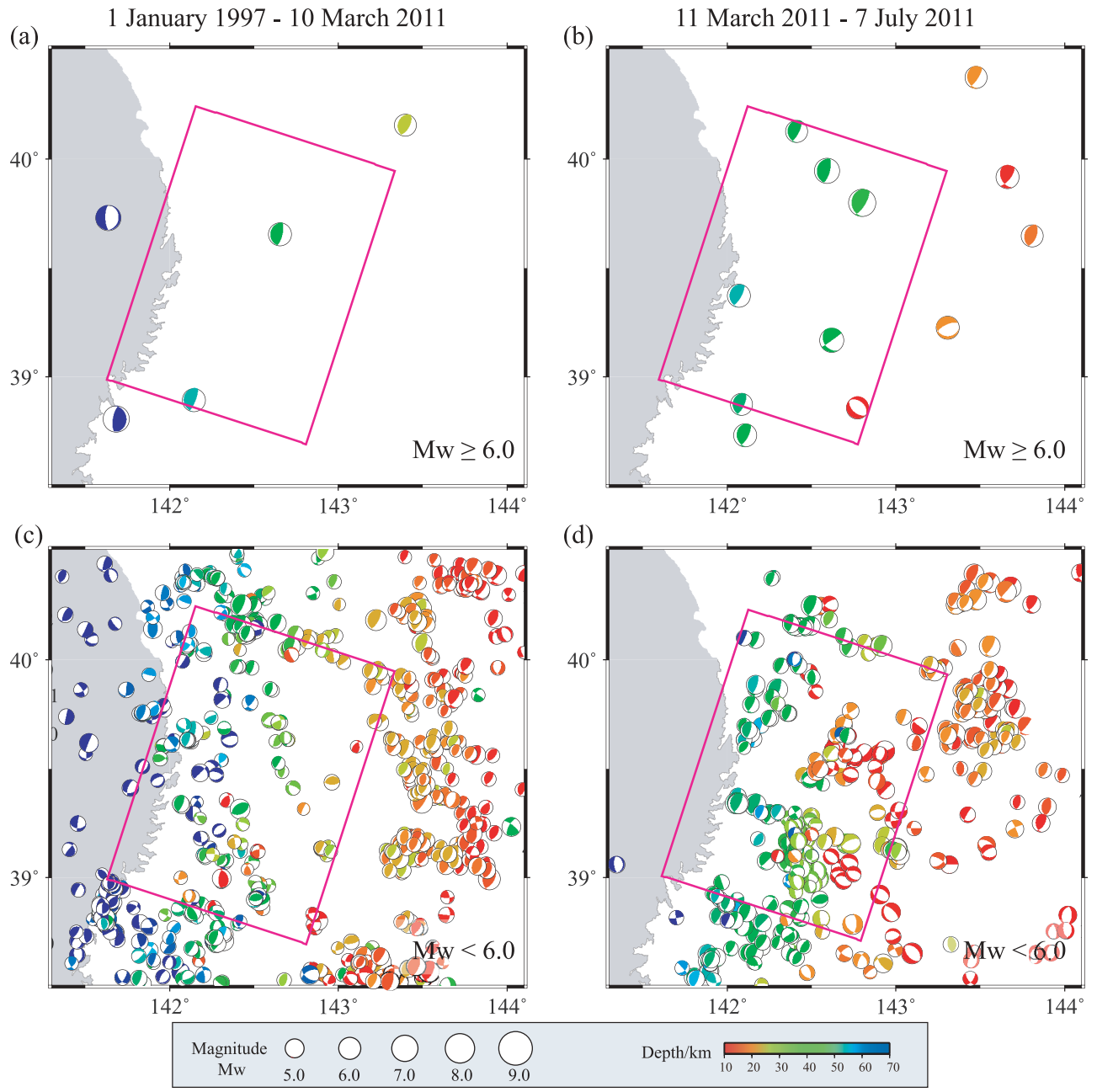

Figure 6. Focal mechanisms from the NIED CMT catalog since 1997 around the SLSR prior to the 11 March 2011 Tohoku-Oki earthquake with (a) $M_w \geq 6.0$ and (b) $M_w < 6.0$, and after the Tohoku-Oki earthquake with (c) $M_w \geq 6.0$ and (d) $M_w < 6.0$. Other symbols are the same as those in Figure 1.

the SLSR margins appear to be interplate thrust events, and there are about a dozen such events within the SLSR prior to 2011 (Figures 5a and 5c) and only a few GCMT events with $M_w > 6.0$ (Figure 5a). The upper plate in the SLSR had some compressional activity prior to the 2011 Tohoku-Oki event, but experienced diffuse extensional activity afterward. Thrust-faulting aftershocks occurred in the northern region of the 1896 rupture zone and in the downdip SLSR region just offshore of the coastline (Figures 5b and 5d), with a cluster near the off-Kamaishi repeater zone at 39.4°N, 142.2°E (Figures 5d).

[18] The NIED moment tensors (Figure 6) are based on inversion of broadband waveforms from F net stations and provide many more solutions for events as small as $M_w = 3.2$. There are differences in M_w between the GCMT and NIED solutions, and 50% more NIED $M_w > 6$ events are apparent for the aftershock sequence (compare Figures 5b and 6b). Many of the NIED mechanisms for lower M_w values located in the SLSR before 2011 (Figure 6c) appear to be intraplate events within the Pacific plate (most blue mechanisms), including a prominent sequence near 38.9°N, 141.8°E. There are again only a few large events with thrusting mechanisms within the SLSR before 2011 relative to the surrounding regions.

[19] The expanded sampling of small aftershock mechanisms provided by the NIED catalog (Figure 6d) indicates

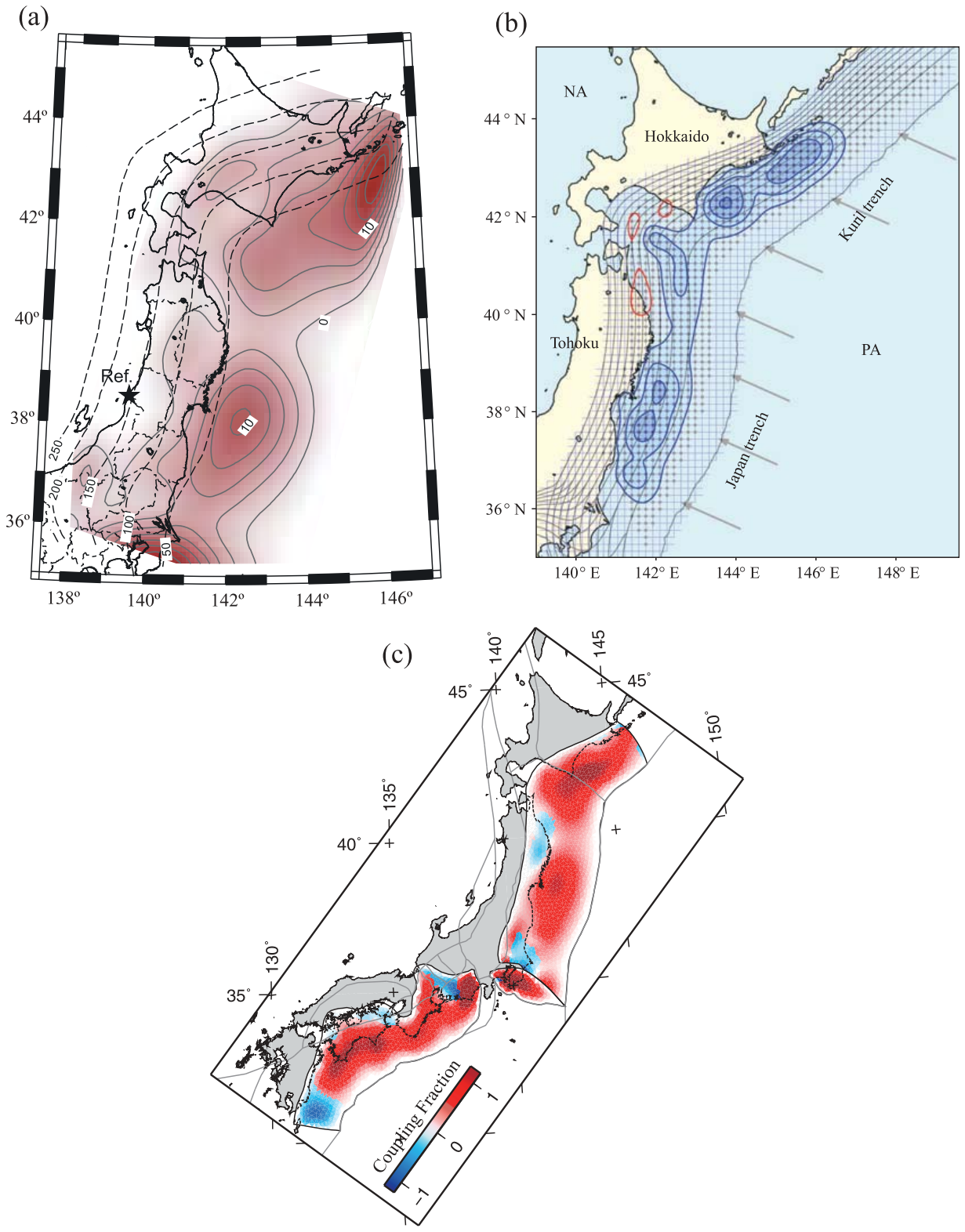

Figure 7. Slip deficit maps. (a) Distribution of back slip rate estimated by inverting three-dimensional velocity data with a contour interval of 2 cm/yr with continuous GPS data from 1997 to 2001. Dashed lines indicate the slab depth every 50 km (modified from *Suwa et al.* [2006]). (b) The distribution of slip-deficit rates (blue contours) and slip-excess rates (red contours) inverted with the GPS data between 1996 and 2000 (modified from *Hashimoto et al.* [2009]). (c) Coupling fraction estimated from GPS observation from 1997 to 2000. A zone of large thrust sense slip around the SLSR may reflect postseismic deformation triggered by 1994 M_w 7.7 Sanriku-Oki earthquake. Thin gray lines indicate the block geometry (modified from *Loveless and Meade* [2010]).

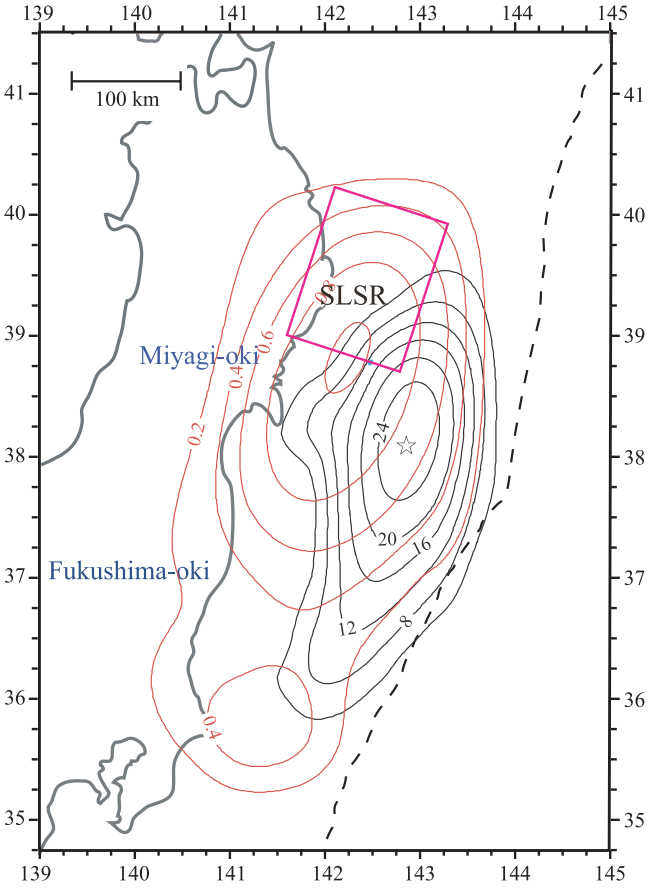

Figure 8. Coseismic slip (black lines, 4 m interval, 10–11 March 2011) and postseismic slip (red lines, 0.2 m interval, 12–25 March 2011) distribution of the 2011 Tohoku-Oki estimated from GPS observation [*Ozawa et al.*, 2011].

several 20 km scale subregions with underthrusting aftershocks in the SLSR close to the coastline (including the off-Kamaishi events), with most events eastward of 142.5° having extensional faulting that is likely located within the upper wedge. The overall activity levels in the SLSR are clearly elevated for the 4 month interval after the 11 March 2011 event, and several of the patches with thrusting aftershocks had only experienced a few events in the preceding decades. The concentration of NIED underthrusting aftershocks in the northern region of the 1896 zone (Figures 6b and 6d) is similar to the GCMT pattern (Figures 5b and 5d). It is interesting that so few underthrusting aftershocks are found south of 39.5°N and east of 142.5°E, as a very large coseismic slip occurred just to the south of this region during the 2011 rupture (Figure 1b).

2.2. Interplate Slip Deficit Around the SLSR

[20] Observations from the dense nationwide global positioning system (GPS) network (GEONET) in Japan since 1996 revealed the crustal strain distribution in Honshu prior to the 2011 Tohoku-Oki earthquake, and this has been modeled by several groups to estimate the spatial distribution of offshore interplate coupling. While estimates of the spatial slip deficit across the megathrust are dependent on assumptions and boundary conditions in the modeling, particularly regarding the degree of coupling allowed at shallow megathrust depths near the trench [*Loveless and Meade*, 2011], any slip deficit on the plate boundary 30–50 km deep in the SLSR should be relatively well resolved because of proximity to the GPS network. Figure 7 shows examples of spatial distributions of inverted "back slip" (the slip deficit required to account for the crustal strain while fully accommodating overall plate convergence) translated into degree of locking around the SLSR.

[21] Assessment of any slip deficit in the SLSR is made more difficult by the coseismic and postseismic deformation of large events like the 1989 (M_w 7.4), 1992 (M_w 6.9), and 1994 (M_w 7.7) Sanriku-Oki events [*Heki et al.*, 1997; *Kawasaki et al.*, 2001; *Yamanaka and Kikuchi*, 2004] east or north of the SLSR. *Nishimura et al.* [2000] regard the SLSR as a region of slip velocity strengthening (aseismic) due to the unusually large postseismic displacement on the megathrust following the 1992 and 1994 earthquakes and the lack of historical large earthquakes. The distribution of the back slip rate in the SLSR during 1997–2001 estimated by *Suwa et al.* [2006] is ~2 cm/yr lower than that in the surrounding region (Figure 7a). *Hashimoto et al.* [2009] argue that slip-deficit zones are the potential source regions of large interplate earthquakes ($M_w \geq 7.5$) and infer that the smaller slip deficit found for GPS data from 1996 to 2000 (Figure 7b) indicates a low likelihood of large earthquakes in the SLSR. *Loveless and Meade* [2010] estimated forward slip of up to 2.5 cm/yr and very low coupling on the subduction zone interface beneath northernmost Honshu in and around the SLSR (Figure 7c). They attribute part of the deformation signal in GPS data from 1997 to 2000 to postseismic dislocation triggered by the 1994 Sanriku-Oki earthquake, giving the forward slip indicated by negative (blue) values.

[22] Overall, GPS inversions for back slip rate distribution and/or postseismic deformation in northeastern Japan prior to the great 2011 earthquake indicated strong megathrust coupling in two large regions off Tokachi north of the SLSR and off Miyagi south of the SLSR, with relatively weak plate coupling in the SLSR (Figure 7). Inversions for back slip tend to be heavily smoothed, and the SLSR is not resolved to have zero slip deficit, just a reduced slip deficit relative to adjacent regions. Specific testing of the hypothesis that there is zero slip deficit could be performed using the seismically defined spatial extent of the SLSR in the future. Given the available inversion models and accepting that there is some lateral smearing of the strains caused by the adjacent region with up to 100% slip deficit (totally locked) that ruptured in the great 2011 event, the geodetic observations indicate that the SLSR has relatively low slip deficit as a result of aseismic displacement involving either stable sliding or episodic slow slip events.

3. The 2011 Main Shock Effects

3.1. Coseismic Slip and Postseismic Slip in the SLSR in 2011

[23] Several coseismic finite-faulting slip distribution models for the 11 March 2011 Tohoku-Oki earthquake have now been inverted for using teleseismic, geodetic, and tsunami data [e.g., *Ammon et al.*, 2011; *Ito et al.*, 2011; *Lay et al.*, 2011b; *Ozawa et al.*, 2011; *Shao et al.*, 2011; *Simons et al.*,

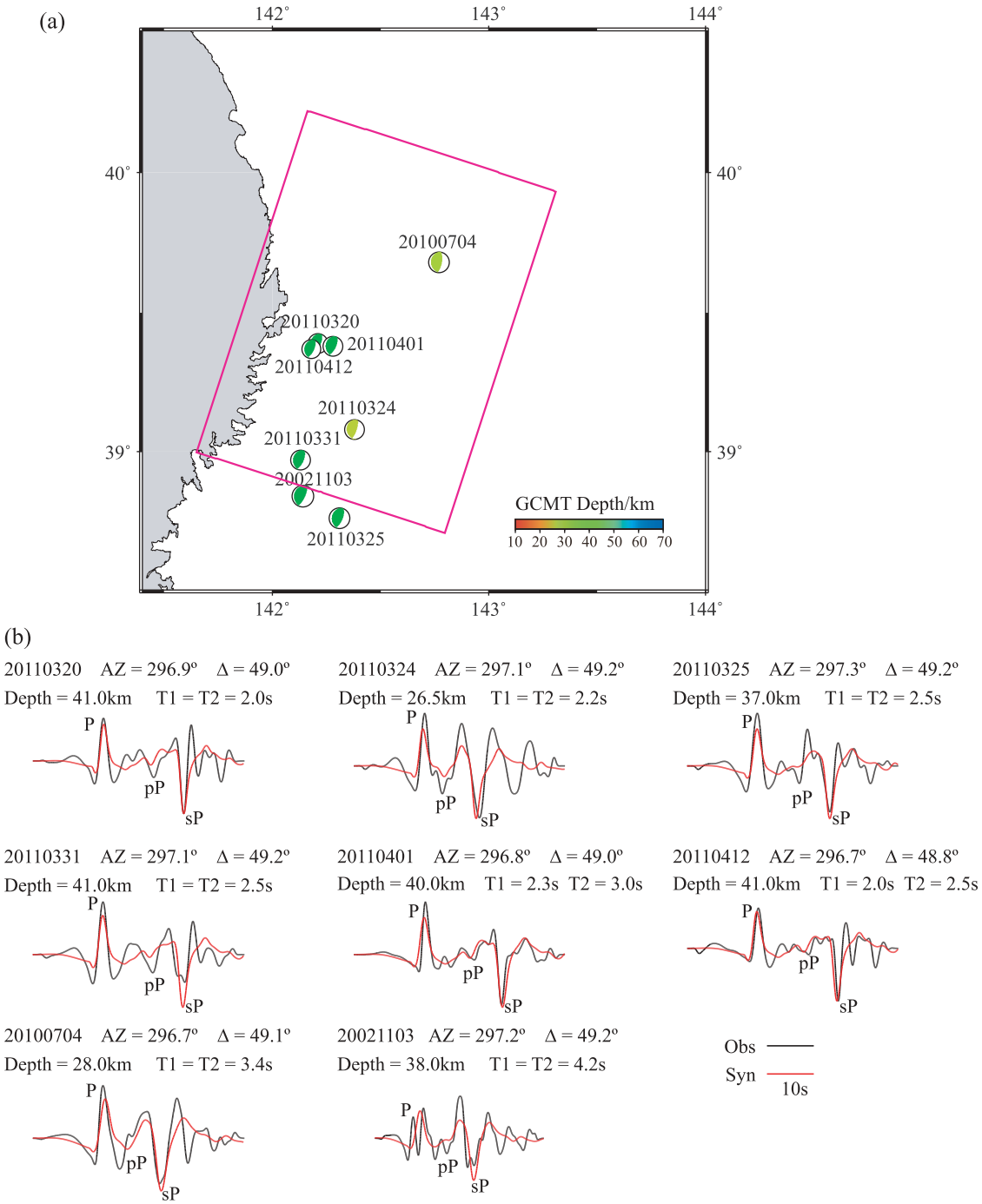

Figure 9. (a) The GCMT location and focal mechanism of the thrusting aftershocks used in waveform modeling in section 3.2. Other symbols are the same as those in Figure 1. (b) Observed (black lines) and synthetic (red lines) teleseismic *P*, *pP*, and *sP* waves for aftershocks in Figure 9a recorded at the station KN.TKM2. The azimuth, epicentral distance, preferred depth, and preferred trapezoidal source duration for each record are indicated above each waveform.

2011]. These models have notable differences, but they are consistent in indicating minor slip on the order of zero to a few meters of coseismic slip in the southern SLSR (e.g., Figures 1 and 8). It appears that despite the SLSR lacking large previous seismic events, it was able to delimit the great 2011 event's northern rupture extent either because of lack of accumulated strain energy available to tap or because of high frictional strength.

[24] On the other hand, GPS data indicate that the post-seismic slip following the 2011 Tohoku-Oki event is largest in the SLSR, on the order of 0.4–0.8 m (Figure 8) [*Ozawa et al.*, 2011]. The lack of coseismic slip and concentration

Table 1. Aftershocks Selected for Waveform Modeling

	Origin Time/UT	Latitude (°N)	Longitude (°E)	Depth (km)				M_w
				PDE	GCMT	JMA	Modeling	
1	2011 03 20 12:03:46.72	39.35	141.82	42.0	55.3	47.8	41.0	5.8
2	2011 03 24 08:21:00.14	39.08	142.08	27.0	37.1	33.7	26.5	5.9
3	2011 03 25 11:36:24.49	38.77	141.88	39.0	51.0	44.7	37.0	6.2
4	2011 03 31 07:15:30.19	38.92	141.82	42.0	54.0	47.4	41.0	6.0
5	2011 04 01 11:57:54.39	39.32	141.95	41.0	52.7	45.2	40.0	5.9
6	2011 04 12 19:37:48.29	39.37	141.90	45.0	56.6	48.3	41.0	5.6
7	2002 11 03 03:37:42.07	38.89	141.98	39.0	44.0	45.8	39.0	6.4
8	2010 07 04 21:55:51.98	39.70	142.37	27.0	35.3	34.5	28.0	6.3

of postseismic slip in the SLSR indicates frictional conditions that are generally unfavorable for seismic failure. However, some aftershocks did occur in the SLSR.

3.2. Large Aftershocks in the SLSR

[25] As shown above, there are relatively numerous aftershocks located in the SLSR compared with preceding activity. About ∼22.5 min after the main shock, an M_w 7.4 (39.84°N, 142.78°E; JMA) aftershock (strike = 179°; rake = 60°; dip = 23°; depth = 35 km from NIED focal mechanism, shown in Figure 6b) occurred near the northeastern corner of the SLSR. This is located close to the 1 November 1989 M_w 7.4 event (39.84°N, 142.76°E, NEIC) event (the GCMT centroid location, 39.95°N, 143.08°E is just inside the SLSR in Figure 5a). The 1989 event has been analyzed by *Yamanaka and Kikuchi* [2004] and *Uchida et al.* [2004]. That event ruptured close to a prior event on 21 March 1960 (M_w 7.3), possibly with overlapping rupture area [*Yamanaka and Kikuchi*, 2004], so the 2011 M_w = 7.4 aftershock is not in a surprising location. Both the 1960 and 1989 events were followed by large aftershock sequences in the shallow megathrust region updip of the SLSR [*Yamanaka and Kikuchi*, 2004].

[26] Numerous moderate-size underthrusting aftershocks (M_w ∼5.0–6.5) have occurred on the downdip portion of the SLSR about 40 km beneath the coastal margin (Figures 5b, 5d, 6b, 6d), with activity extending along the length of the SLSR, but clustered in 2–3 groups. There is very little aftershock thrust activity from 142.5°E–143.25°E. Numerous normal-fault events occurred at upper plate depths in this eastern portion of the SLSR, but only the downdip portion appears to have had thrust aftershocks.

[27] We modeled teleseismic *P* waves for the larger recent thrust events in and near the SLSR to confirm the source depths and to evaluate whether they had unusual rupture characteristics. Adequate broadband teleseismic *P* wave data were found for six aftershocks (M_w 5.9–6.2) and 2 earlier events (M_w 6.3–6.4) with low dip angle faults and hypocentral depths consistent with interplate events (Figure 9). A few *P* wave recordings at azimuths of ∼300° with high signal-to-noise ratios were forward modeled, holding the GCMT mechanism fixed and varying the source depth and source duration.

[28] The depths of most larger thrust events (Table 1) are determined to be ∼40 km except the 4 July 2010 event (depth = 28.0 km) located northeast of the other events. The modeling depth estimates are consistent with those from the JMA unified and NEIC catalogs and shallower than the GCMT centroid depths by ∼15 km. The *P* wave signals used have weak *pP* arrivals compared with *sP*, which is consistent with the focal mechanisms having low dip angles of ∼19°–26°. In each case ∼2–3 s trapezoidal source durations provide good matches to the *P* waveforms. This duration is typical of M_w 6.0 events, and these SLSR events do not show any distinctive waveforms relative to comparably sized events elsewhere, and the aftershocks are not distinctive from the earlier events. The 3 November 2002 event has complex double-pulse *P* waves, but we do not model the details, as we mainly wanted to confirm the depth.

3.3. Repeating Earthquakes Off Kamaishi

[29] Seven underthrusting aftershocks with M_w 4.3–5.9 occurred on the plate boundary offshore of Kamaishi (∼39.4°N, ∼142.0°E) where the M_j 4.8 ± 0.1 repeating earthquake sequence was observed by *Matsuzawa et al.* [2002]. To identify whether they are repeating earthquakes of this sequence, we calculated the cross correlation of the waveforms of these seven aftershocks with those for earlier identified repeating earthquakes in 2001 and 2008 [*Okada et al.*, 2003; *Shimamura et al.*, 2011]. We used signals recorded by the broadband network *F* net in Japan for the time window from 10 s before predicted *P* arrival to 10 s after predicted *S* wave arrival. Waveform cross correlations indicate that at least two of the events, events 13 and 15 in Table 2 (group A), are precisely colocated with earlier off-Kamaishi repeating events in 2001 and 2008. The other four events, 11, 12, 14, and 16 (group B) show high waveform similarity with each other but are clearly somewhat different from the earlier repeaters. Also, the magnitudes of these events (M_j = 5.3–5.9) are consistently larger than those of earlier repeating events (M = 4.7–5.1) and events 13 and 15. An increase in size of repeaters and initiation of new repeater sequences were observed for the 2004 Parkfield earthquake as well [*Chen et al.*, 2010]. Event 17 has few high cross-correlation coefficients with the signals for the two groups, so it appears distinctive.

[30] Even though there appear to be at least two groups based on waveform similarities, cross-correlation coefficients between events from the two groups are still ∼0.8 for the most nearby stations. Since digital data for the off-Kamaishi repeating sequence are available at our stations for only the 2001 and 2008 events, it is hard to evaluate definitively whether the events in group B and event 17 are or are not repeaters of prior events in the off-Kamaishi group. The

Table 2. Possible Repeating Earthquakes Off-Kamaishi

Event	Origin Time (JST)	Latitude (°N)	Longitude (°E)	Depth (km)	Magnitude (M_j)
1	1957 09 27, 21:43:27.20	39.3170	142.0000	49.0	4.9
2	1962 07 30, 19:51:04.30	39.3330	142.0670	50.0	4.9
3	1968 10 17, 22:28:22.50	39.3000	142.1170	50.0	4.9
4	1973 12 08, 06:07:21.80	39.3330	142.0500	50.0	4.8
5	1979 07 19, 10:30:00.20	39.3500	141.9330	50.0	4.8
6	1985 03 01, 11:35:06.00	39.3430	142.0520	51.0	4.9
7	1990 07 16, 21:35:10.00	39.3400	142.0420	52.0	5.0
8	1995 03 11, 13:49:56.90	39.3250	142.1220	57.1	5.1
9	2001 11 13, 16:45:05.40	39.3370	142.0690	48.0	4.8
10	2008 01 11, 08:00:31.70	39.3410	142.0670	47.2	4.7
11	2011 03 11, 15:40:49.50	39.3260	142.0720	51.4	5.7
12	2011 03 20, 21:03:47.50	39.3440	142.0480	47.8	5.9
13	2011 03 29, 08:51:31.10	39.3440	142.0550	49.1	4.3
14	2011 04 13, 04:37:48.40	39.3440	142.0650	48.3	5.5
15	2011 04 29, 15:54:48.10	39.3400	142.0640	48.2	4.8
16	2011 05 31, 21:28:35.70	39.3420	142.0620	48.0	5.3
17	2011 07 11, 13:29:28.38	39.3417	142.0605	50.0	5.1

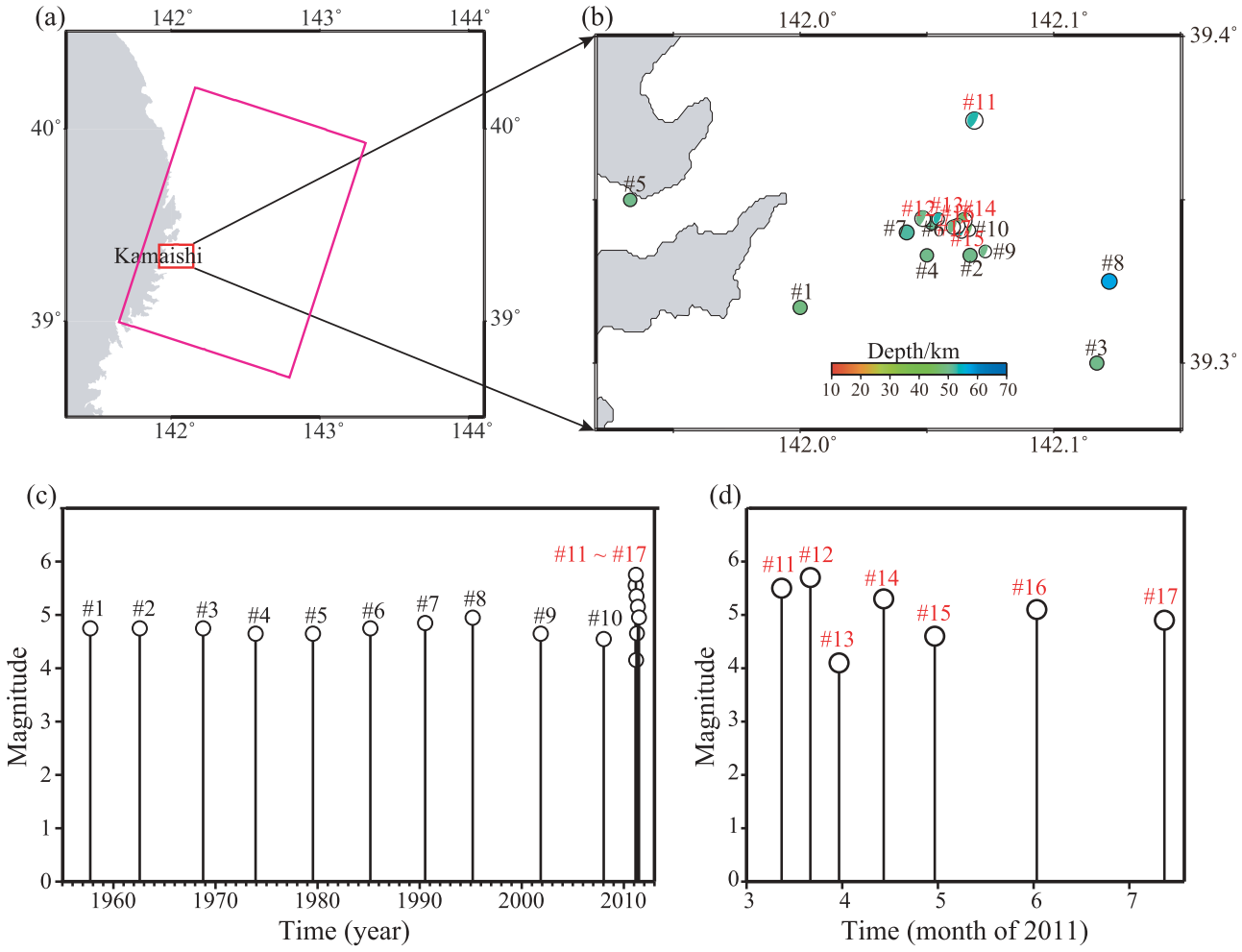

Figure 10. (a) Location of the region of the off-Kamaishi repeater sequence (red box) within the SLSR (magenta box) (b) Locations from the JMA unified catalog of 7 aftershocks with M_w 4.3–5.9 off Kamaishi and 10 earthquakes in the M 4.8 ± 0.1 repeating sequences there [*Matsuzawa et al.*, 2002]. (c) Magnitude versus time diagram of all 17 events. (d) Expanded time scale of the aftershock sequence.

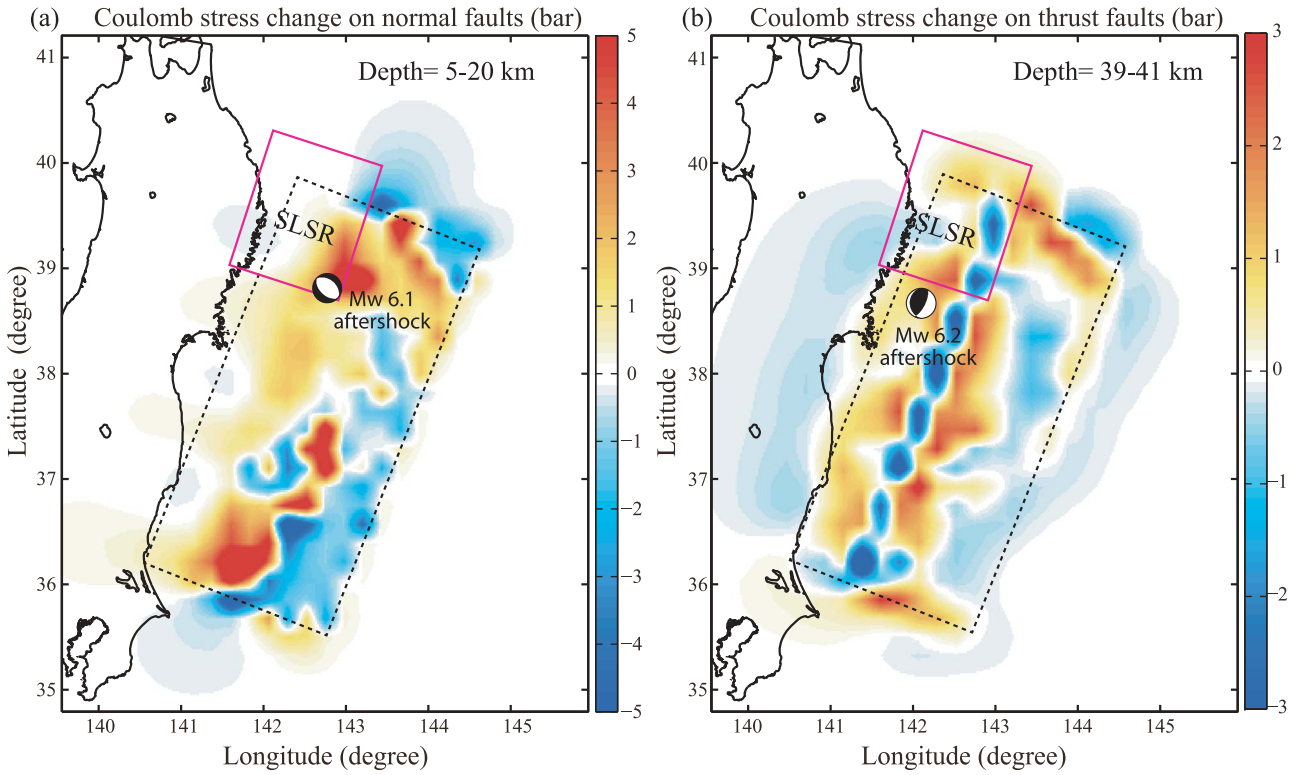

Figure 11. Maps of Coulomb stress change predicted for the coseismic slip model from *Yue and Lay* [2011]. (a) The Coulomb stress change averaged over the depth range 5–20 km for normal-faulting geometry given by the westward dipping plane of an M_w 6.1 aftershock located in the SLSR (11 March 2011, 20:11 UTC; strike = 140°, dip = 41°, rake = −76°; NIED CMT solution). (b) The Coulomb stress change over the depth range 39–41 km for a shallow-dipping thrust-faulting geometry given by an M_w 6.2 aftershock (25 March,11:36:28.2 UTC; strike = 185°; dip = 26°; slip = 74°; NIED CMT solution), which is the largest aftershock modeled in section 3.1.

occurrence of at least two definite repeating earthquakes, events 13 and 15, supports the notion of a local asperity with a size of ∼1 km loaded to failure by steady sliding of the surrounding megathrust [*Matsuzawa et al.*, 2002]. Since the other events are very similar to each other and may be repeats of earlier off-Kamaishi events, it appears that the large postseismic deformation following the great 2011 earthquake accelerated the repeated failure of one or two asperities rather dramatically (Figure 10).

3.4. Stress Changes in the SLSR Thrust Zone

[31] The limited and localized occurrence of thrusting aftershocks indicates that most of the postseismic deformation in the SLSR is taking place aseismically. Evaluating the stress perturbation produced by the main shock displacement can give some guidance on the stress changes in the SLSR. We used Coulomb 3 software (provided by S. Toda, R. Stein, J. Lin, and V. Sevilgen) to estimate the stress perturbation for the coseismic slip model from *Yue and Lay* [2011] (Figure 1b), obtained by inversion of high-rate GPS observations across Honshu. A friction coefficient of 0.4 was assumed, but the results are not particularly sensitive to this choice for the range 0.2–0.8. We calculated the average stress change over the depth range 5–20 km for the southwestward dipping fault plane of a normal faulting geometry (Figure 11a) given by an M_w 6.1 aftershock located in the SLSR (11 March 2011, 20:11 UTC; strike = 140°, dip = 41°, rake = −76°; NIED CMT solution) and the average stress change over the depth range 39–41 km for a shallow-dipping thrust-faulting geometry (Figure 11b) of an M_w 6.2 aftershock (25 March 2011, 11:36:28.2 UTC; strike = 185°; dip = 26°; slip = 74°; NIED CMT solution), which is the largest aftershock modeled in section 3.1. For shallow normal faulting, the driving stress increased by ∼5 bars in the SLSR, which is compatible with the occurrence of numerous extensional aftershocks in the upper plate (Figures 5 and 6). At greater depth within the SLSR near the megathrust, the driving stress for thrusting increased ∼3 bars near the coastline, which is consistent with the band of thrusting aftershocks in the SLSR discussed above. Not all aftershocks are in regions of strong Coulomb stress increase for their focal mechanism, but this may result from differences in depth or inaccuracy of the slip model, as well as other factors that influence seismicity.

[32] Coulomb stress calculations provide only first-order guidance with respect to changes in the SLSR stress environment, as the ambient stresses are not known. However, the general shift from compressional activity to extensional activity in the intraplate environment (Figure 6) does suggest relatively low stress [e.g., *Hasegawa et al.*, 2011]. Thus, aseismic convergence may be inferred to be occurring in the

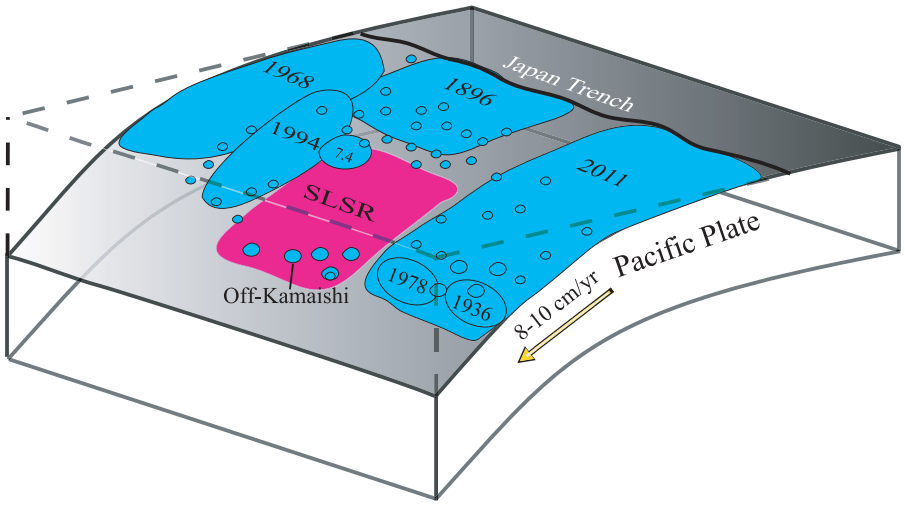

Figure 12. Schematic map of the Japan megathrust fault showing the distribution of rupture zone of historic large events and the 2011 Tohoku earthquake (large blue regions), and aftershocks (small blue regions) along the megathrust from Japan Trench. We plot the southern end of the 1896 rupture zone as extending to about 39°N, north of the aseismic zone seen in Figure 2e, consistent with the southern extent of the tsunami model of *Aida* [1977] and the region of strong inundation on the Iwate coast indicated by *Hatori* [1974]. The convergence velocity of the Pacific Plate is indicated by a yellow arrow. The magenta region highlights the SLSR on the megathrust. The SLSR is largely aseismic, but does have modest-size patches of seismogenic regions downdip, including the off-Kamaishi repeater zone. The shallower portion of the SLSR is almost devoid of moderate-size thrust events, but seismic activity is high in the 1896 rupture zone region further updip.

region because of low frictional resistance rather than as a result of very high stress stable sliding.

4. Discussion and Conclusions

[33] Source process analysis of large earthquakes and interplate coupling distribution estimated from GPS observation for northeast Japan provide support for an asperity model characterization of the SLSR megathrust (Figure 12), as has been suggested by *Yamanaka and Kikuchi* [2004], *Hashimoto et al.* [2009], and *Uchida and Matsuzawa* [2011]. The deeper portion of the SLSR has moderate-size thrust events, in concentrated patches both before and after the 2011 Tohoku-Oki main shock. These patches normally failed at a slow rate before the great 2011 event, but the rate increased after the event. This is particularly clear for the off-Kamaishi repeating earthquake sequence in which two confirmed repeaters, and many additional events on a nearby asperity, occurred within 4 months after the main shock. This increase in failure rate is generally consistent with the predicted Coulomb stress change for models of the main shock slip and with the concentration of postseismic deformation in the vicinity of the SLSR. The updip portion of the SLSR megathrust has very few thrusting events, and the total seismic moment of thrusting for the whole SLSR constitutes a tiny fraction of plate convergence slip.

[34] Postseismic slip is accelerated creep following a main shock and is generally thought to happen on weak or stably sliding areas of the fault in response to increased strain rate in the main shock vicinity. The <5 m slip during the 2011 rupture and the ~0.4–0.8 m postseismic slip in the SLSR support the idea that the region is weakly coupled and that resulting low strain accumulation may have served as an elastic energy sink that bounded the 2011 rupture. The high ratio of the number of repeating earthquakes to the total number of earthquakes [*Igarashi et al.*, 2003] and the fringing of the SLSR by slow slip events, such as accompanied the 1989 Sanriku-Oki (M_w 7.4), 1992 Sanriku-Oki (M_w 6.9), and 1994 Sanriku-Oki (M_w 7.7) earthquakes, indicate that little strain has accumulated in the SLSR with convergence having been accommodated by aseismic slip. It is likely that this region is either totally decoupled or is in a velocity-strengthening state given the lack of induced thrust-faulting aftershocks.

[35] The cause of the distinct nature of the frictional state on the SLSR relative to adjacent regions of the megathrust is unclear. There is evidence for volumetric velocity heterogeneity in the vicinity of the 2011 Tohoku-Oki large slip zone, where relatively high V_p is observed [*Zhao et al.*, 2011] and in the transition from large updip slip to lower downdip slip [*Kennett et al.*, 2011], where low shear velocity and low bulk sound velocity are observed. The latter study, along with that by *Zhao et al.* [2009], finds low velocities near the megathrust in the upper portion of the SLSR as well, with an increase in the ratio downdip below the coastline. The presence of fluids could reduce the shear velocity and possibly the frictional strength in the aseismic region of the SLSR, but specific causes of the frictional behavior are not known.

[36] The updip region of the Ibaraki-Oki megathrust region to the south of the 2011 rupture zone has some similar attributes to the SLSR. While the downdip region has had historical $M > 7+$ events, such as the 1938 sequence with cumulative seismic moment equivalent to $M_w \sim 8.1$ [*Abe*, 1977], the updip activity in this region is low (Figure 2). Relatively low back slip and low slip deficit in the downdip

region have also been estimated in this region (Figure 7c) [*Loveless and Meade*, 2010]. A large underthrusting aftershock (M_w 7.9) occurred in the downdip megathrust (36.18°N, 141.17°E) ~30 min after the Tohoku-Oki earthquake [e.g., *Lay et al.*, 2011a], but the updip region from 35°–36°N, 141.2°–142.2°E appears not to have had coseismic slip and had relatively few aftershocks (Figure 2). These observations suggest that weak interplate coupling and little strain accumulation might have also bounded the 2011 slip zone to the south in the same way the SLSR appears to have bounded it to the north. The aseismic zone extending from the SLSR to the trench (ellipse in Figures 2e and 2f) may have bounded the extent of updip rupture for the 2011 event and plausibly the southern extent of the 1896 rupture.

[37] The SLSR appears to be a region where great earthquakes will not nucleate and through which they do not manage to rupture. The lines of evidence supporting this interpretation include the low GPS-inferred slip deficit, the lack of historical great events, localized zones of repeating earthquakes that appear to be surrounded by quasi-static deformation and were accelerated by the 2011 rupture, significant 2011 postseismic slip, and lack of triggered thrust aftershocks from adjacent giant earthquake over the updip portion. The occurrence of large postseismic deformation for large earthquakes to the north of the SLSR and slow rupture updip in the 1896 tsunami earthquake, with abrupt transition in microseismicity at about 143°E, further indicate transitions to a distinct frictional regime in the SLSR. The overall evidence suggests that this region is not storing strain that will be released in a future great event, but rather is accommodating most plate convergence with aseismic sliding of most of the SLSR fault surface. Characterizing other regions with similar properties may help to define bounds on adjacent large earthquake ruptures.

[38] **Acknowledgments.** This work made use of GMT and SAC software. Seismic catalogs and focal mechanisms were obtained from JMA, NIED, NEIC, and GCMT. K. Katsumata provided a convenient version of the JMA unified catalog. Y. Asano kindly provided a copy of his unpublished focal mechanism catalog of regional CMT inversions. N. Uchida shared his catalog of repeating events in the Japan Trench. B. L. N. Kennett provided a preprint of his velocity tomography results. C. Ammon provided seismicity maps that motivated this examination of the SLSR. We thank an anonymous reviewer and T. Matsuzawa for comments that improved the manuscript. This work was supported by NSF grant EAR0635570.

References

Abe, K. (1977), Tectonic implications of the large Shioya-Oki earthquakes of 1938, *Tectonophysics*, *41*, 269–289, doi:10.1016/0040-1951(77)90136-6.

Abe, K. (1979), Size of great earthquakes of 1873–1974 inferred from tsunami data, *J. Geophys. Res.*, *84*, 1561–1568, doi:10.1029/JB084iB04p01561.

Aida, I. (1977), Simulations of large tsunamis occurring in the past off the coast of the Sanriku district [in Japanese], *Bull. Earthquake Res. Inst. Univ. Tokyo*, *52*, 71–101.

Ammon, C. J., T. Lay, H. Kanamori, and M. Cleveland (2011), A rupture model of the 2011 off the Pacific coast of Tohoku Earthquake, *Earth Planets Space*, *63*, 693–696, doi:10.5047/eps.2011.05.015.

Asano, Y., T. Saito, Y. Ito, K. Shiomi, H. Hirose, T. Matsumoto, S. Aoi, S. Hori, and S. Sekiguchi (2011), Spatial distribution and focal mechanisms of aftershocks of the 2011 off the Pacific coast of Tohoku Earthquake, *Earth Planets Space*, *63*, 669–673, doi:10.5047/eps.2011.06.016.

Chen, K. H., R. Burgmann, R. M. Nadeau, T. Chen, and N. Lapusta (2010), Postseismic variations in seismic moment and recurrence interval of small repeating events following the 2004 Parkfield earthquake, *Earth Planet. Sci. Lett.*, *299*, 118–125, doi:10.1016/j.epsl.2010.08.027.

Earthquake Research Committee (1998), *Seismic Activity in Japan.* 222 pp., Headquarters for Earthquake Research Promotion, Prime Minister's Office, Tokyo, Japan.

Gamage, S. S. N., N. Umino, A. Hasegawa, and S. H. Kirby (2009), Offshore double-planed shallow seismic zone in the NE Japan forearc region revealed by sP depth phases recorded by regional networks, *Geophys. J. Int.*, *178*, 195–214, doi:10.1111/j.1365-246X.2009.04048.x.

Hasegawa, A., K. Yoshida, and T. Okada (2011), Nearly complete stress drop in the 2011 M_w 9.0 off the Pacific coast of Tohoku Earthquake, *Earth Planets Space*, *63*, 703–707, doi:10.5047/eps.2011.06.007.

Hashimoto, C., A. Noda, T. Sagiya, and M. Matsu'ura (2009), Interplate seismogenic zones along the Kuril–Japan trench inferred from GPS data inversion, *Nat. Geosci.*, *2*, 141–144, doi:10.1038/ngeo421.

Hatori, T. (1974), Tsunami sources on the Pacific side in northeast Japan [in Japanese], *J. Seism. Soc. Jpn.*, *2*(27), 321–337.

Heki, K., S. I. Miyazaki, and H. Tsuji (1997), Silent fault slip following an interplate thrust earthquake at the Japan Trench, *Nature*, *386*, 595–598, doi:10.1038/386595a0.

Igarashi, T., T. Matsuzawa, and A. Hasegawa (2003), Repeating earthquakes and interplate aseismic slip in the northeastern Japan subduction zone, *J. Geophys. Res.*, *108*(B5), 2249, doi:10.1029/2002JB001920.

Ito, T., K. Ozawa, T. Watanabe, and T. Sagiya (2011), Slip distribution of the 2011 off the Pacific coast of Tohoku Earthquake inferred from geodetic data, *Earth Planets Space*, *63*, 627–630, doi:10.5047/eps.2011.06.023.

Kanamori, H. (1971), Seismological evidence for a lithospheric normal faulting–The Sanriku earthquake of 1933, *Phys. Earth Planet. Inter.*, *4*, 289–300, doi:10.1016/0031-9201(71)90013-6.

Kanamori, H. (1972), Mechanism of tsunami earthquakes, *Phys. Earth Planet. Inter.*, *6*, 346–359, doi:10.1016/0031-9201(72)90058-1.

Kanamori, H. (1977), Seismic and aseismic slip along subduction zones and their tectonic implications, in *Island Arcs, Deep Sea Trenches and Back-Arc Basins*, *Maurice Ewing Ser.*, vol. 1, edited by T. Talwani and W. C., Pitman, pp. 163–174, AGU, Washington, D. C., doi:10.1029/ME001.

Kanamori, H., M. Miyazawa, and J. Mori (2006), Investigation of the earthquake sequence off Miyagi prefecture with historical seismograms, *Earth Planets Space*, *58*, 1533–1541.

Kawasaki, I., Y. Asai, and Y. Tamura (2001), Space-time distribution of interplate moment release including slow earthquakes and the seismo-geodetic coupling in the Sanriku-oki region along the Japan trench, *Tectonophysics*, *330*, 267–283.

Kennett, B. L. N., A. Gorbatov, and E. Kiser (2011), Structural controls on the Mw 9.0 2011 Offshore-Tohoku earthquake, *Earth Planet. Sci. Lett.*, *310*, 462–467, doi:10.1016/j.epsl.2011.08.039.

Lay, T., C. J. Ammon, H. Kanamori, M. J. Kim, and L. Xue (2011a), Outer trench-slope faulting and the 2011 M_w 9.0 off the Pacific coast of Tohoku Earthquake, *Earth Planets Space*, *63*, 713–718, doi:10.5047/eps.2011.05.006.

Lay, T., C. J. Ammon, H. Kanamori, L. Xue, and M. J. Kim (2011b), Possible large near-trench slip during the 2011 M_w 9.0 off the Pacific coast of Tohoku Earthquake, *Earth Planets Space*, *63*, 687–692, doi:10.5047/eps.2011.05.033.

Loveless, J. P., and B. J. Meade (2010), Geodetic imaging of plate motions, slip rates, and partitioning of deformation in Japan, *J. Geophys. Res.*, *115*, B02410, doi:10.1029/2008JB006248.

Loveless, J. P., and B. J. Meade (2011), Spatial correlation of interseismic coupling and coseismic rupture extent of the 2011 M_w = 9.0 Tohoku-oki earthquake, *Geophys. Res. Lett.*, *38*, L17306, doi:10.1029/2011GL048561.

Matsuzawa, T., T. Igarashi, and A. Hasegawa (2002), Characteristic small-earthquake sequence off Sanriku, northeastern Honshu, Japan, *Geophys. Res. Lett.*, *29*(11), 1543, doi:10.1029/2001GL014632.

Matsuzawa, T., N. Uchida, T. Igarashi, T. Okada, and A. Hasegawa (2004), Repeating earthquakes and quasi-static slip on the plate boundary east off northern Honshu, Japan, *Earth Planets Space*, *56*, 803–812.

Mazzotti, S., X. Le Pichon, P. Henry, and S. I. Miyazaki (2000), Full interseismic locking of the Nankai and Japan-west Kurile subduction zones: An analysis of uniform elastic strain accumulation in Japan constrained by permanent GPS, *J. Geophys. Res.*, *105*, 13159–13177, doi:10.1029/2000JB900060.

Minoura, K., F. Imamura, D. Sugawara, Y. Kono, and T. Iwashita (2001), The 869 Jogan tsunami deposit and recurrence interval of large-scale tsunami on the Pacific coast of northeast Japan, *J. Nat. Disaster Sci.*, *23*, 83–88.

Nishimura, T., S. Miura, K. Tachibana, K. Hashimoto, T. Sato, S. Hori, E. Murakami, T. Kono, K. Nida, and M. Mishina (2000), Distribution of seismic coupling on the subducting plate boundary in northeastern Japan inferred from GPS observations, *Tectonophysics*, *323*, 217–238, doi:10.1016/S0040-1951(00)00108-6.

Okada, T., T. Matsuzawa, and A. Hasegawa (2003), Comparison of source areas of M4.8 ± 0.1 repeating earthquakes off Kamaishi, NE Japan: Are asperities persistent features? *Earth Planet. Sci. Lett.*, *213*, 361–374, doi:10.1016/S0012-821X(03)00299-1.

Ozawa, S., T. Nishimura, H. Suito, T. Kobayashi, M. Tobita, and T. Imakiire (2011), Coseismic and postseismic slip of the 2011 magnitude-9 Tohoku-Oki earthquake, *Nature*, *475*, 373–376, doi:10.1038/nature10227.

Satake, K., Y. Sawai, M. Shishikura, Y. Okamura, Y. Namegaya, and S. Yamaki (2007), Tsunami source of the unusual AD 869 earthquake off Miyagi, Japan, inferred from tsunami deposits and numerical simulations of inundation, *Eos Trans. AGU*, *88*(23), Fall Meeting Suppl., Abstract T31G–03.

Shao, G., X. Li, C. Ji, and T. Maeda (2011), Focal mechanism and slip history of the 2011 M_w 9.1 off the Pacific coast of Tohoku Earthquake, constrained with teleseismic body and surface waves, *Earth Planets Space*, *63*, 559–564, doi:10.5047/eps.2011.06.028.

Shimamura, K., T. Matsuzawa, T. Okada, N. Uchida, T. Kono, and A. Hasegawa (2011), Similarities and differences in the rupture process of the $M\sim$4.8 repeating-earthquake sequence off Kamaishi, Northeast Japan: Comparison between the 2001 and 2008 events, *Bull. Seismol. Soc. Am.*, *101*, 2355–2368, doi:10.1785/0120100295.

Simons, M., et al. (2011), The 2011 magnitude 9.0 Tohoku-Oki Earthquake: Mosaicking the megathrust from seconds to centuries, *Science*, *332*, 1421–1425, doi:10.1126/science.1206731.

Suwa, Y., S. Miura, A. Hasegawa, T. Sato, and K. Tachibana (2006), Interplate coupling beneath NE Japan inferred from three-dimensional displacement field, *J. Geophys. Res.*, *111*, B04402, doi:10.1029/2004JB003203.

Tanioka, Y., and K. Satake (1996), Fault parameters of the 1896 Sanriku tsunami earthquake estimated from tsunami numerical modeling, *Geophys. Res. Lett.*, *23*, 1549–1552, doi:10.1029/96GL01479.

Uchida, N., and T. Matsuzawa (2011), Coupling coefficient, hierarchical structure, and earthquake cycle for the source area of the 2011 Tohoku earthquake inferred from small repeating earthquake data, *Earth Planets Space*, *63*, 675–679, doi:10.5047/eps.2011.07.006.

Uchida, N., T. Matsuzawa, A. Hasegawa, and T. Igarashi (2003), Interplate quasi-static slip off Sanriku, NE Japan, estimated from repeating earthquakes, *Geophys. Res. Lett.*, *30*(15), 1801, doi:10.1029/2003GL017452.

Uchida, N., A. Hasegawa, T. Matsuzawa, and T. Igarashi (2004), Pre-and post-seismic slow slip on the plate boundary off Sanriku, NE Japan associated with three interplate earthquakes as estimated from small repeating earthquake data, *Tectonophysics*, *385*, 1–15, doi:10.1016/j.tecto.2004.04.015.

Uchida, N., J. Nakajima, A. Hasegawa, and T. Matsuzawa (2009), What controls interplate coupling?: Evidence for abrupt change in coupling across a border between two overlying plates in the NE Japan subduction zone, *Earth Planet. Sci. Lett.*, *283*, 111–121, doi:10.1016/j.epsl.2009.04.003.

Watanabe, H. (2001), Realities of the 869 Jogan earthquake and tsunami and the inferred tsunami source, *Hist. Earthquakes*, *14*, 83–99.

Wyss, M., C. G. Sammis, R. M. Nadeau, and S. Wiemer (2004), Fractal dimension and *b*-value on creeping and locked patches of the San Andreas fault near Parkfield, California, *Bull. Seismol. Soc. Am.*, *94*(2), 410–421, doi:10.1785/0120030054.

Yamanaka, Y., and M. Kikuchi (2004), Asperity map along the subduction zone in northeastern Japan inferred from regional seismic data, *J. Geophys. Res.*, *109*, B07307, doi:10.1029/2003JB002683.

Yue, H., and T. Lay (2011), Inversion of high-rate (1 sps) GPS data for rupture process of the 11 March 2011 Tohoku earthquake (M_w 9.1), *Geophys. Res. Lett.*, *38*, L00G09, doi:10.1029/2011GL048700.

Zhao, D., Z. Wang, N. Umino, and A. Hasegawa (2009), Mapping the mantle wedge and interplate thrust zone of the northeast Japan arc, *Tectonophysics*, *467*, 89–106, doi:10.1016/j.tecto.2008.12.017.

Zhao, D., Z. Huang, N. Umino, A. Hasegawa, and H. Kanamori (2011), Structural heterogeneity in the megathrust zone and mechanism of the 2011 Tohoku-oki earthquake (Mw 9.0), *Geophys. Res. Lett.*, *38*, L17308, doi:10.1029/2011GL048408.

H. Kanamori, Seismological Laboratory, California Institute of Technology, Pasadena, CA 91125, USA.

T. Lay and L. Ye, Department of Earth and Planetary Sciences, University of California, Santa Cruz, CA 95064, USA. (tlay@ucsc.edu)